Computer Assisted Mechanics and Engineering Sciences, 3: 389–401, 1996.

Error estimation for FEM in acoustic scattering

Dedicated to the memory of Prof. dr. habil. inż. Marian Kmiecik

Frank Ihlenburg*
Texas Institute for Computational and Applied Mathematics,
The University of Texas at Austin

(Received April 10, 1996)

We consider apriori and aposteriori error estimation for the FEM solution of Helmholtz problems that arise in acoustic scattering. Our focus is on the case of high wavenumber (highly oscillatory solutions) where existing asymptotic estimates had to be generalized to "preasymptotic" statements that are applicable in the range of engineering computations. We refer the key results of an 1D analytic study of error behavior (apriori estimates) and announce new results on aposteriori error estimation. Specifically, we show that the standard local aposteriori error indicators are not, in general, reliable for Helmholtz problems with high wave number, due to considerable numerical pollution in the error. We then discuss a methodology how to (aposteriori) estimate, in addition to the local error, the pollution error. Throughout, the theoretical results will be supplemented by numerical evaluation.

1. Introduction

The reliable identification of submarine objects is a topic of continued interest in naval research. The physical problem is, in the frequency domain, formulated as an exterior boundary value problem (BVP) for the Helmholtz equation (rigid acoustic scattering) or a coupled system of Helmholtz equations (elastic scattering), respectively.

Analytical solutions for Helmholtz BVP (or, equivalently, for the Helmholtz integral equations) are feasible for regular shapes of the scatters, whereas numerical methods are applied in the general case. We assume in this paper that a domain decomposition of the exterior domain is applied for the numerical solution as depicted in Fig. 1:

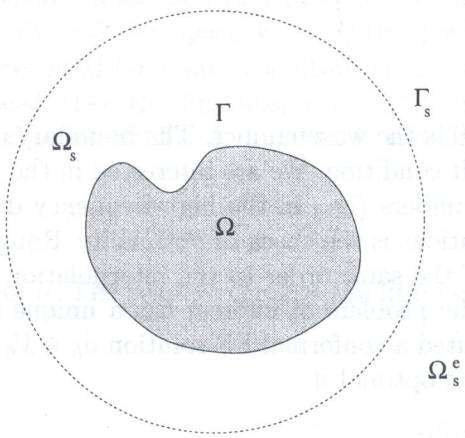

Fig. 1. Scatterer within a unit sphere

*TICAM, Taylor Hall 2,400, UT at Austin, Austin, TX 78712, U.S.A.; ihl@ticam.utexas.edu

The rigid scatterer Ω is enclosed by a regular smooth artificial boundary Γ_s (specifically, we assume that the physical object has been scaled such that it is fitted into the unit sphere). The annular region Ω_s between the scatterer and the artificial boundary is discretized by standard h-p finite elements. For concreteness and in accord with our numerical evaluation, we assume that the region Ω_s^e exterior to the artificial boundary Γ_s is divided into infinite elements. The focus of this paper is on the quality and reliability of the FEM-discretization in the annulus, hence the choice of the numerical method in the exterior is optional. The FEM could be coupled as well with the BEM, DtN-condition or another method of numerical approximation. We consider here only the case of rigid scattering. For related results on the FEM in elastic scattering, see [12, 11].

Here, we give a survey of published and unpublished results on error estimation for oscillatory solutions that are typical in acoustics. We elaborate on the problems of apriori and aposteriori error estimation in separate sections. We hope to give the reader an understanding of the tight interlink that exists between these two approaches of error estimation. While aposteriori estimation of the error is the subject that is certainly most important in engineering applications, a deep understanding of the error behavior and thus a judgement about the reliability of the aposteriori estimates is usually gained from apriori analysis. In the case of the Helmholtz equation, the most important feature is the pollution effect that dominates the quality of the finite element solution for high wavenumber. The notion of this effect was introduced in [8]; here, we show also how pollution of the FE error affects the quality of local indicators in aposteriori error estimation.

The analytical results are given for a very simple 1D model problem. As an applied example of 3D calculations, we present in section 4 numerical results for the rigid scattering of a plane wave from a sphere. It will be seen that the error behavior in the 3D computations for the Helmholtz equation shows the same numerical effects as studied in the 1D model problem. To our knowledge, this is the first numerical investigation of the FEM error in 3D computations for the Helmholtz equation. For a study of the FEM for 2D Helmholtz equation, see [2, 10].

The investigations were motivated by numerical problems that surfaced while the author was involved in a research project of the U.S. Office of Naval Research which also partly funded the author's stay at the University of Maryland at College Park.

2. THE POLLUTION EFFECT IN FEM-SOLUTIONS OF HELMHOLTZ EQUATION — APRIORI ESTIMATES

For analytical purpose, we consider the following most simple one-dimensional model problem. Let $\Omega = (0,1)$ be the unit interval and find the complex-valued solution u of the BVP

$$\begin{aligned} u''(x) + k^2 u(x) &= -f(x)\,, \\ u(0) &= 0\,, \\ u'(1) - iku(1) &= 0\,, \end{aligned} \tag{1}$$

where the real parameter $k > 0$ is the wavenumber. The boundary condition at $x = 1$ is equivalent to a non-reflecting Sommerfeldt condition. We are interested in the performance of FE-solutions to this problems for large wavenumbers (i.e., in the high-frequency domain). A standard method to measure the quality of FE-solutions is the check of optimality. Roughly, a finite element solution is called optimal if its error is of the same order as the interpolation error in the discrete subspace. More precisely, assume that the problem of interest has a unique solution in a function space V and that there has been computed a conformal FE solution $u_h \in V_h \subset V$ (i.e., u_h lies in a subspace of V). The FE solution is called optimal if

$$\|u - u_h\|_V \leq C \inf_{v_h \in V_h} \|u - v_h\|_V \tag{2}$$

holds for a constant C that does not depend on the choice of the subspace (i.e., on the numerical parameter h — the meshsize of the FEM). For our analysis of the Helmholtz problem, we require

that all constants of error estimation are also independent of the physical parameter k. The choice of the meshsize h is a delicate question in discrete solutions of Helmholtz' equation. The reason lies in the oscillatory behavior of the exact solution. Let us illustrate this on the model problem. The fundamental solutions to the ordinary differential equation are the sine and cosine functions $\{\sin kx, \cos kx\}$. The higher the wavenumber k, the higher are the oscillations of the solutions and the shorter the wavelength $\lambda = 2\pi/k$. It is intuitively clear that a "rule of thumb"

$$n_{\text{res}} = \frac{\lambda}{h} \approx \text{const.} \tag{3}$$

should be applied in the design of the mesh for given k. The number n_{res} is called the *resolution* of the mesh. We illustrate this in Fig. 2 with $n_{\text{res}} = 8$; the choice $n_{\text{res}} = 10$ is usually recommended in practice. However, it is known from computations that the FE error grows with the wavenumber

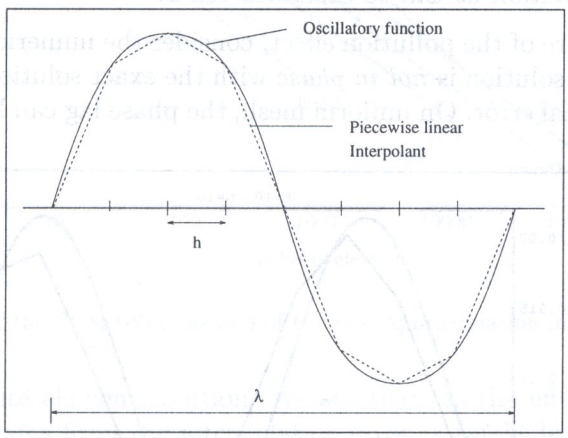

Fig. 2. Resolution of wave — $n_{\text{res}} = 8$

also on meshes where the rule of thumb is satisfied. On the other hand, the error of interpolation of the exact solution (which, of course, is not known in general) is constant for any wavenumber k if the rule (3) is used. Indeed the optimality condition (2) can be proven for the model problem (1) only under the assumption that $k^2 h \ll 1$. For large k, this assumption is much too restrictive for practical computations.

A complete analysis of the FE-error behavior for Helmholtz' equation in the range of practical computation, $hk = \text{const.}$, has been given in [8, 9, 10]. Here, we refer only the results for the classical h-version from [8]. Since we consider a second-order problem, the natural functional space for the variational (weak) solutions is the Sobolev space $V = H^1_{(o}(0,1)$ where the subscript (o indicates that the functions satisfy the essential boundary condition at $x = 0$. Assume that a FE mesh X_h of stepsize h has been introduced, then the FE-subspace $V_h \subset V$ is the space of piecewise linear, continuous functions with nodal points in X_h. A norm on V is defined by

$$\|u\|_1 = \int_0^1 |u'|^2 \mathrm{d}x\,, \tag{4}$$

where u' is the first derivative of u. The relative error of the finite element solution in this norm is denoted by

$$e_1 = \frac{\|u - u_h\|_1}{\|u\|_1}\,.$$

In [8], we prove — assuming only that $kh < 1$ — the estimate

$$e_1 \leq C_1 kh + C_2 k^3 h^2\,, \tag{5}$$

where C_1, C_2 are constants independent of k, h. The first member on the right hand side of (5) represents the interpolation error (note that this error is bounded if kh is constant). Further, writing the r.h.s. as $Ckh(1+k^2h)$ we see that the estimate (5) reduces to the optimality statement (2) if k^2h is small. However, if this condition is not satisfied then, for large wavenumber, the second term is clearly leading in the estimate (5). We call this term the *pollution term.*

Remark 1: *The notion of numerical pollution is frequently used in the analysis of elasticity problems in domains with geometric singularities like cracks or re-entrant corners. Roughly, we speak of numerical pollution if a considerable part of the error in some local domain of interest (say, some part of an elastic structure that is located at some distance from a singularity) is not measurable and not improvable on that local domain only. In the case of elastic structures, the error throughout the domain depends significantly on the degree of local refinement around the singularity. In the case of Helmholtz problems, the pollution effect is related not to a local singularity but to the phase lag of the finite element solution as will be explained below.*

To understand the nature of the pollution effect, consider the numerical results plotted in Fig. 3. We see that the numerical solution is *not in phase* with the exact solution and that the phase lag is the main source of numerical error. On uniform mesh, the phase lag can be quantified by computing

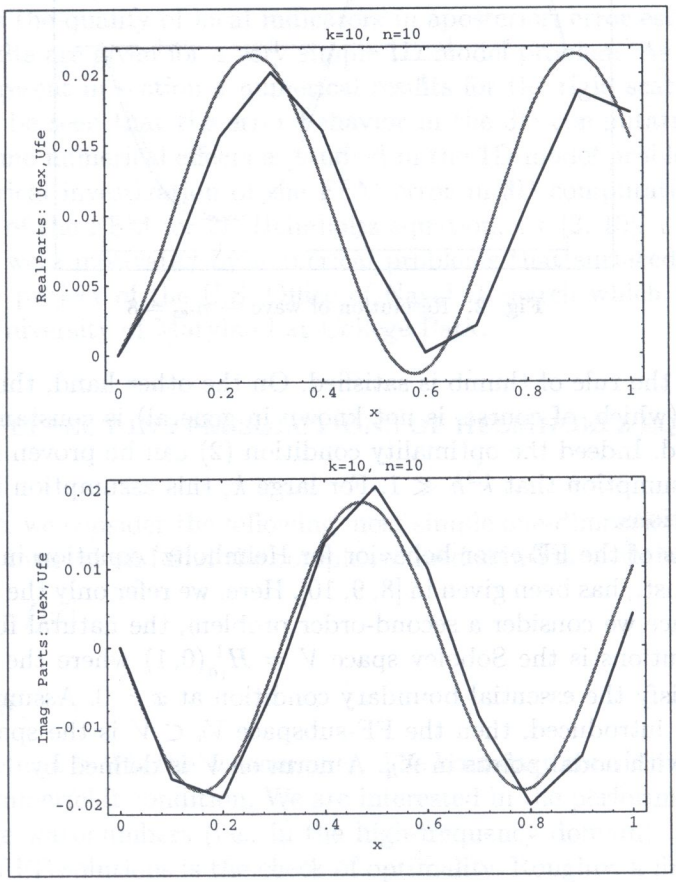

Fig. 3. Phase lag of the finite element solution for $k = 10$, $h = 0.1$

the discrete wavenumber $\tilde{k}$ via discrete Fourier analysis (see, e.g., [13]). In the engineering literature, this approach is frequently called dispersion analysis.

In [9], we prove that, for general h-p-FEM,

$$|\tilde{k} - k| \leq k\, C \left(\frac{C_a(p)}{2}\right)^2 \left(\frac{hk}{2p}\right)^{2p},$$

holds if $kh < 1$, where k is the exact wavenumber, C_a is an approximation constant and C does not depend on k, h and p.

Taking $p = 1$ we see that the phase lag of the p.w. linear FEM is exactly of the same order as the pollution term (this observation generalizes to the h-p FEM, see [9]). In this sense, the results of dispersion analysis and numerical analysis of the Helmholtz equation are equivalent [10].

The foregoing numerical results are illustrated in Fig. 4. The curved lines in the plot show the

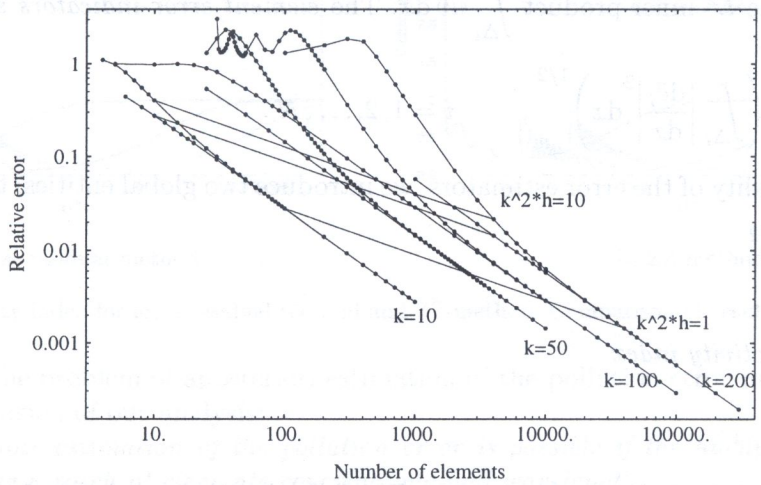

Fig. 4. Relative error of the FEM solutions and of the best approximation in H^1-norm for different k

relative error e_1 of the finite element solution. We see that, as the effect of numerical pollution, this error increasingly deviates from the interpolation error (straight lines below the curved lines) as k grows. On the other hand, the lines connecting different values of k^2h on the FE error and the BA error, respectively, show that indeed the finite element error is optimal if (and only if) k^2h is restricted. Note that we show a log-log-plot, hence constant distance in the plot actually depicts a constant ratio as indicated by the optimality condition (2). All error curves asymptotically decrease with the rate -1. By standard theory of piecewise linear interpolation, the interpolation error satisfies

$$\|u - u_I\|_1 \leq Ch\|u\|_2 ,$$

where the norm $\|u\|_2$ is defined by replacing the first derivative with the second derivative in (4). Since $h = N^{-1}$, the rate -1 is to be expected as N (number of elements) is plotted on the abcissa.

3. The problem of aposteriori error estimation for Helmholtz' equation

We have seen in the preceeding paragraph that the error of the finite element solution for Helmholtz' equation is increasingly polluted for large wavenumber unless the mesh is extremely refined. In practice, one is most interested in accurate and reliable methods of aposteriori error estimation. In the analysis of large structures, typically the error has to be estimated only in some local region of particular interest. Several methods have been proposed for local aposteriori error estimation. Here, we analyse a method based on the solution of local residual problems. We will then see in numerical examples that the results apply to the local smoothening method (ZZ-estimator, [14]) as well. Let us introduce the usual local notations. On an arbitrary element Δ_i, we define the *interior residuum*

$$r_{\Delta_i} := \left(-f - \frac{\mathrm{d}^2 u_h}{\mathrm{d}x^2} - k^2 u_h\right)\Big|_{\Delta_i} . \tag{6}$$

We then define the element *residual indicator function* $\hat{e}_i \in H_o^1(\Delta_i)$ as the solution of the variational problem: Find $\hat{e}_i \in H_o^1(\Delta_i)$ such that

$$B_{\Delta_i}(\hat{e}_i, \hat{v}) := \left(\frac{\mathrm{d}\hat{e}_i}{\mathrm{d}x}, \frac{\mathrm{d}\hat{v}}{\mathrm{d}x}\right)_{\Delta_i} - k^2(\hat{e}_i, \hat{v})_{\Delta_i} = (r_{\Delta_i}, \hat{v})_{\Delta_i}, \qquad \forall\, \hat{v} \in H_o^1(\Delta_i), \tag{7}$$

where $H_o^1(\Delta_i)$ denotes the subspace of H^1-functions that vanish on the element boundaries and $(u, v)_{\Delta_i}$ denotes the L^2 inner product $\int_{\Delta_i} u\bar{v}\,\mathrm{d}x$. The *element error indicators* are given by

$$\eta_i := |\hat{e}_i|_{1,\Delta_i} = \left(\int_{\Delta_i} \left|\frac{\mathrm{d}\hat{e}_i}{\mathrm{d}x}\right|^2 \mathrm{d}x\right)^{1/2}, \qquad i = 1, 2, \ldots, N. \tag{8}$$

To measure the quality of the error estimators, we introduce two global entities: the *global estimator*

$$\mathcal{E} := \left(\sum_{i=1}^{N} \eta_i^2\right)^{1/2} \tag{9}$$

and the *global effectivity index*

$$\kappa := \frac{\mathcal{E}}{|e_h|_{1,\Omega}}. \tag{10}$$

Desirably, the effectivity index is close to one. The following theorem holds [1], cf. also [7]:

Theorem: *Assume $kh < \pi$. Then*

$$\frac{1}{\left(1 + \dfrac{k^2h}{\pi}\right)\left(1 + \left(\dfrac{kh}{\pi}\right)^2\right)} \leq \kappa \leq \frac{1 + C(1+k)\dfrac{k^2h^2}{\pi}}{\left(1 - \left(\dfrac{kh}{\pi}\right)^2\right)}$$

holds with

$$C = \frac{2}{\left(1 - 2(1+k)\dfrac{k^2h^2}{\pi^2}\right)\pi},$$

provided k, h are such that C is positive.

It will be shown by numerical experiments that the effectivity index is in fact close to the lower bound of the Theorem. Hence the local error indicator significantly *underestimates* the true error for large wavenumber. Only if k^2h is small the effectivity index is close to 1. This is consistent with our analysis in section 2. Indeed, if k is large and k^2h is not small then the numerical error is dominated by the pollution term that, due to its global nature, cannot be measured by *any* method of local aposteriori error estimation.

As an illustration, consider the numerical results shown in Fig. 5. We solve again the 1D model problem (1) of section 2. The error of the FEM is estimated aposteriori by the local residual method and the smoothening method proposed by Zienkiewicz and Zhu [14]. The first observation is that both local indicators lead to similar behavior of the error estimators and effectivity indices. In accord with the Theorem, the effectivity indices tend to 1 asymptotically (if k^2h is sufficiently small); however, for large k, the error indicators significantly *underestimate* the true error on the meshes used in practice (i.e., with $hk = \text{const}$).

Thus it is necessary, for large wavenumber, to use a method for estimation of the pollution error that complements the standard local estimators. This method should be again local, i.e., the estimate of the pollution error should be computable only in some region of interest, using the already computed FE-solution as data.

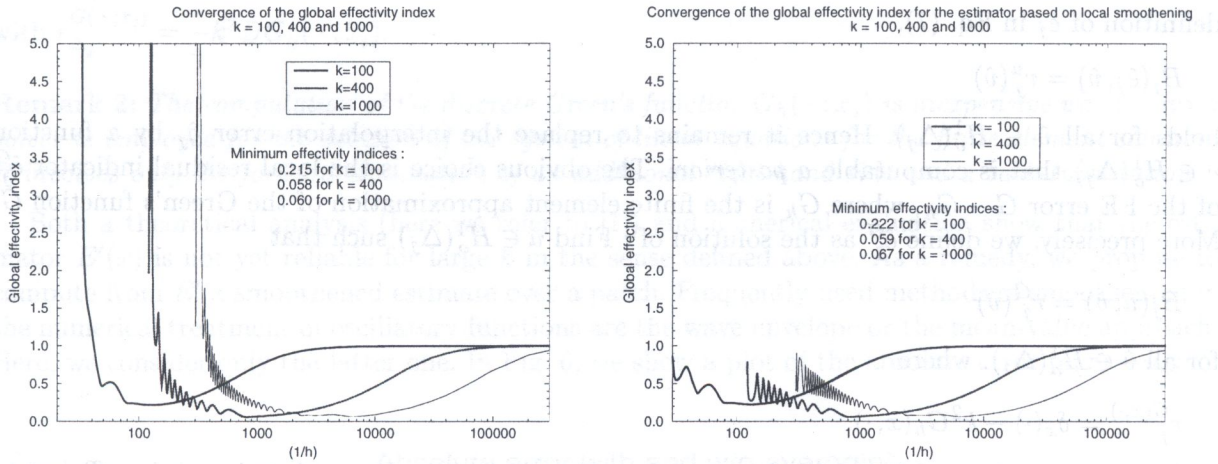

a) Local residual method b) ZZ method

Fig. 5. Effectivity index for local residual method and ZZ-method. Comparison of results for different k

We investigate the problem of aposteriori estimation of the pollution error in [1]. Here, we only refer the main conlusion of our analysis:

Reliable aposterioir estimation of the pollution error is possible if the highly oscillatory waves are smoothened over a patch of elements covering one-half wavelength.

By reliable error estimation, we mean estimators that have an effectivity index not growing rapidly with k on meshes for which $hk = \text{const}$. Let us shortly introduce our methodology and explain more precisely what mean by "smoothening". The key point in estimation of the pollution error is to use the Green's function of the Helmholtz problem as a test function in the variational formulation.

Consider again the model problem (1) or, equivalently, the weak formulation: Find $u \in V$ such that

$$B(u,v) = (f,v) \tag{11}$$

holds for all $v \in V$, where

$$B(u,v) = \int_0^1 \left(u'(x)\bar{v}'(x) - k^2 u(x)\bar{v}(x)\right) \mathrm{d}x - iku(1)\bar{v}(1) \tag{12}$$

and $(f,v) = \displaystyle\int_0^1 f(x)\bar{v}(x)\,\mathrm{d}x$. By definition of the Green's function, $B(w(\cdot), \bar{G}(x,\cdot)) = w(x)$ for all $w \in V$. Taking $w = e_h = u - u_h$ we have, in particular,

$$e_h(x) = B(e_h(s), \bar{G}(x,s)) = B(e_h(s), \bar{G}(x,s) - v_h(s)) \tag{13}$$

for all $v_h \in V_h$. Here, we used the fact that the finite element error is B-orthogonal to all functions from the FE-subspace V_h. Choosing $v_h = \mathcal{I}_h^1 \bar{G}$ (piecewise linear interpolant of $\bar{G}$), and denoting $\hat{g} = G - \mathcal{I}_h^1 G$, we have

$$\begin{aligned} e_h &= B(e_h, \bar{\hat{g}}) = \sum_{j=1}^{N} B_j(e_h, \bar{\hat{g}}_j) \\ &= \sum_{j=1}^{N} r_j^u(\bar{\hat{g}}_j) = \sum_{j=1}^{N} B_j(\hat{e}_j, \bar{\hat{g}}_j), \end{aligned}$$

where $\hat{e}_j$ is the local residual indicator of the FE-error, $\hat{g}_j$ is the restriction of $\hat{g}$ to the element Δ_j and $r^u = f - \mathrm{d}^2 u_h/\mathrm{d}x^2 - k^2 u_h$ is the interior local residuum defined in Eq. (6). Note that, by

definition of $\hat{e}_j$ in Eq. (7),

$$B_j(\hat{e}_j, \hat{v}) = r_j^u(\hat{v})$$

holds for all $\hat{v} \in H_o^1(\Delta_j)$. Hence it remains to replace the interpolation error $\hat{g}_j$ by a function $\hat{v} \in H_o^1(\Delta_j)$ that is computable *a posteriori*. The obvious choice is the local residual indicator $\hat{e}_j^G$ of the FE error $G - G_h$, where G_h is the finite element approximation of the Green's function G. More precisely, we define $\hat{e}_j^G$ as the solution of : Find $\hat{u} \in H_o^1(\Delta_j)$ such that

$$B_j(\hat{u}, \hat{v}) = r_j^G(\hat{v})$$

for all $\hat{v} \in H_o^1(\Delta_j)$, where

$$r_j^{G(x,\cdot)} = \delta_x(\cdot) - k^2 G_h(x, \cdot).$$

Since we already established local aposteriori estimates for the element interiors, it is sufficient to compute the pollution estimate in *just one point* of each element Δ_j. We choose the right boundary of each element by fixing $x = x_j$ for computation of the pollution error in the element Δ_j.

Resuming, we obtain the entity

$$E(x_i) := \sum_{\substack{j=1 \\ j \neq i}}^{N} B_{\Delta_j}\left(\hat{e}_j, \bar{\hat{e}}_j^{G(\cdot\,, x_i)}\right), \tag{14}$$

where $\hat{e}_j^{G(\,\cdot\,;x_i)} \in H_0^1(I_j)$ satisfies

$$B_{\Delta_j}\left(\hat{e}_j^{G(\,\cdot\,;x_i)}, \hat{v}\right) = \left(r_{\Delta_j}^{G(\,\cdot\,;x_i)}, \hat{v}\right)_{\Delta_j}, \qquad \hat{v} \in H_0^1(\Delta_j), \qquad 1 \leq j \leq N$$

with $r_{\Delta_j}^{G(\,\cdot\,;x_i)}(\,\cdot\,) = -k^2 G_h(\,\cdot\,; x_i)$. Note that the Dirac function in the residual is skipped here since the evaluation is done in nodal points and the functional r acts only on functions that vanish in the nodal points.

The element of interest is left out in the summation since the pollution error is evaluated on the outside of the element. Similarly to $E(x)$, we define an estimator for $\dfrac{\mathrm{d}e_h}{\mathrm{d}x}(\bar{x}_i)$, where $\bar{x}_i = \dfrac{x_i + x_{i-1}}{2}$ is the midpoint of element Δ_i, as follows:

$$\frac{\mathrm{d}e_h}{\mathrm{d}x}(\bar{x}_i) \simeq \frac{e_h(x_i) - e_h(x_{i-1})}{h} = B(e_h, \overline{DG}(\,\cdot\,; x_i)),$$

where $DG(\,\cdot\,;\bar{x}_i) := \dfrac{1}{h}\Big(G(\,\cdot\,;x_i) - G(\,\cdot\,;x_{i-1})\Big)$. As before, we have the equality

$$\frac{\mathrm{d}e_h}{\mathrm{d}x}(\bar{x}_i) = \sum_{\substack{j=1 \\ j \neq i}}^{N} B_{\Delta_j}(\hat{e}_j, \overline{DG - \mathcal{I}_h DG}). \tag{15}$$

Replacing the interpolation error $DG - \mathcal{I}_h DG$ by the FEM solution $\hat{e}^{DG}$, we get an *estimator for the derivative* of the error at $\bar{x}_i$:

$$E'(\bar{x}_i) = \sum_{\substack{j=1 \\ j \neq i}}^{N} B_{\Delta_j}\left(\hat{e}_j, \bar{\hat{e}}_j^{DG(\,\cdot\,;\bar{x}_i)}\right), \tag{16}$$

where $\hat{e}_j^{DG(\,\cdot\,;\bar{x}_i)} \in H_0^1(\Delta_j)$ satisfies

$$B_{\Delta_j}\left(\hat{e}_j^{DG(\,\cdot\,;\bar{x}_i)}, \hat{v}\right) = \left(r_{\Delta_j}^{DG(\,\cdot\,;\bar{x}_j)}, \hat{v}\right)_{\Delta_j} \qquad \forall\, \hat{v} \in H_0^1(\Delta_j)$$

with $r_{\Delta_j}^{G(\,\cdot\,;\bar{x}_i)} = -k^2 DG_h(\,\cdot\,;\bar{x}_i)$.

Remark 2: *The computation of the discrete Green's function $G_h(\,\cdot\,;x_j)$ is inexpensive when a direct solver is employed for the solution of the system of linear equations for the finite element solution. It involves only the forward elimination of an additional right-hand side and a back-substitution.*

Both a theoretical analysis (here we refer to [1]) and numerical evaluation show that the estimator $E'(x)$ is not yet reliable for large k in the sense defined above. As a remedy, we propose to compute from E' a smoothened estimate over a patch. Frequently used methods of smoothening in the numerical treatment of oscillatory functions are the wave-envelope or the mean-value approach. Here, we consider only the latter one. In Fig. 6, we show a plot of the absolute error $|u(x) - u_h(x)|$

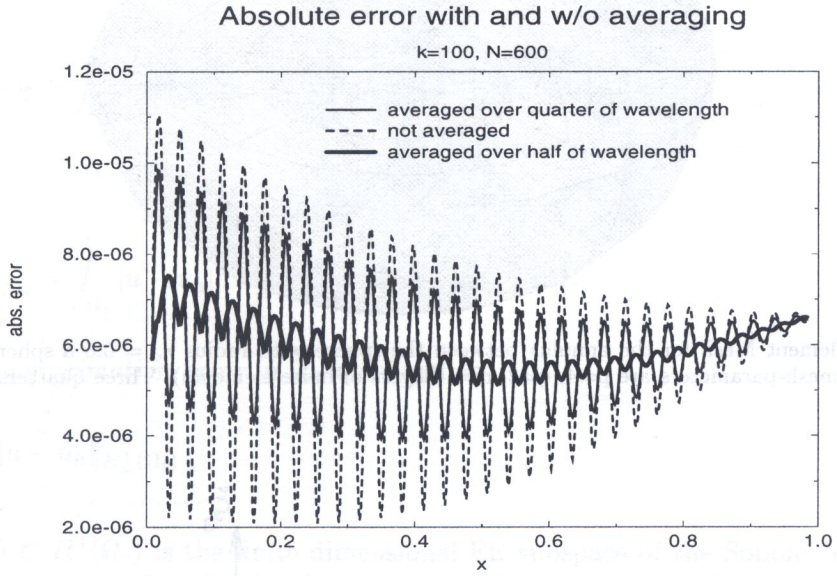

Fig. 6. Smoothed exact error obtained by sliding averages over 1/2 wavelength

for the finite element solution of the model problem (1) for $k = 100$ and $N = 600$ and compare the original error to the smoothened error that is obtained by taking moving averages over one-half wave-length (i.e., we compute in each nodal point x_i the average of all nodal values on the patch, were x_i is taken as the center of the patch). Note the significant reduction of amplitude in the smoothened curve. Furthermore, the smoothened curve is strictly bounded away from zero, preventing distortions in the effectivity index. For the computation of the effectivity index, the smoothened estimator (sliding averages of the elementwise pollution estimators E'_j) is divided by the average of the exact pollution error over the same patch. We can show by numerical experiment that a reliable pollution estimator is obtained by this methodology. Details are given in [2]. For large wavenumber, a patch of one-half wavelength is small compared to the size of the domain and hence the methodology is local as required.

4. Numerical evaluation

As an applied example, consider the 3D problem of scattering of a plane wave from a rigid sphere. For this problem, the exact solution is known and can be used to compute the exact error as well as the error of best approximation. We solve the problem numerically with a coupled FEM-IFEM approach that has been implemented on DEC and IBM workstations at TICAM. The implementation is based on a code that has been developed under the supervision of L. Demkowicz in Kraków and

Austin [3, 4]. Details of the solution procedure and analytical results are given in [6]. The scatterer, a sphere of radius $r_o = 0.5$, is enclosed by an artificial boundary — the surface of the unit sphere, denoted by Γ_s. In the annulus, a 3D finite element discretization is employed — cf. Fig. 7. The master prismatic element, shown in Figure 8, consists of six vertex nodes and fifteen *higher-order*

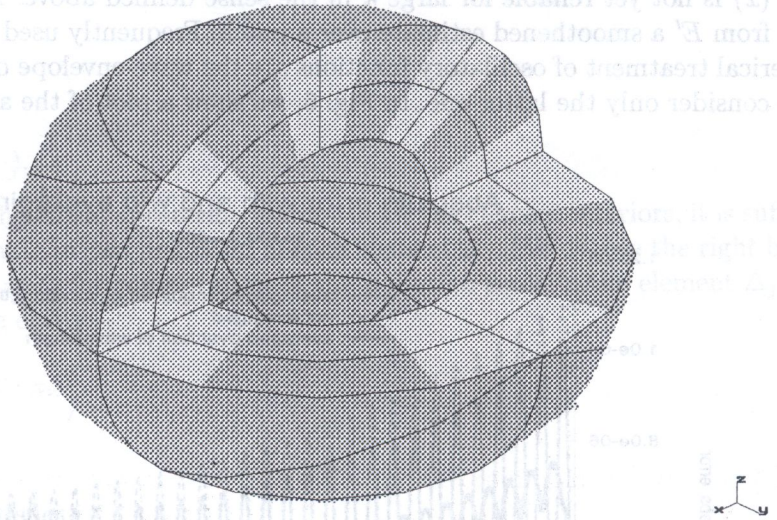

Fig. 7. Finite Element Mesh for the annulus between the sphere with radius $r_o = 0.5$ a sphere within the unit sphere. The mesh-parameters are p=4, q=2, n=2 (layers of finite elements). Three quarters of the mesh are displayed

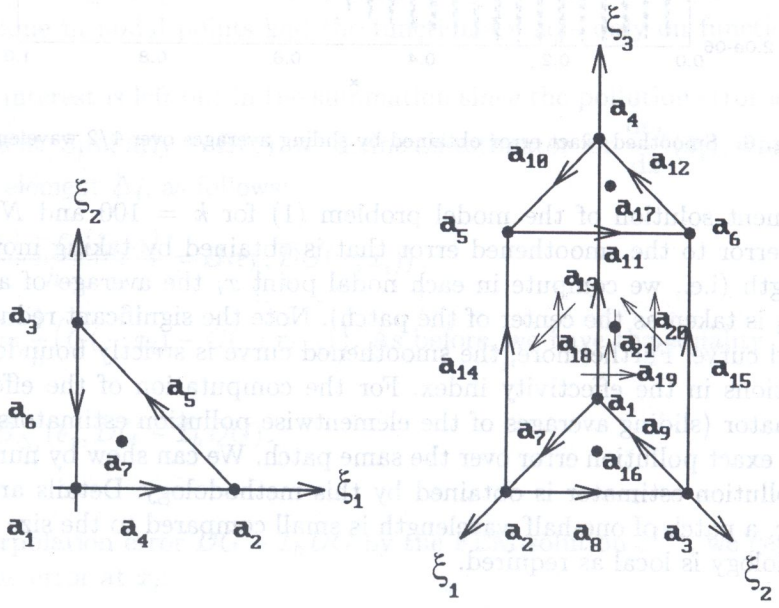

Fig. 8. Master triangle and master prism

nodes: nine *mid-edge*, two *mid-base*, three *mid-side* and one *middle* node. The corresponding shape functions are tensor products of the 2D triangle shape functions $\varphi_i(\xi_1, \xi_2)$ and 1D *incremental* shape functions $\varphi_j(\xi_3)$

$$\varphi_k(\xi_1, \xi_2, \xi_3) = \varphi_i(\xi_1, \xi_2) \cdot \varphi_j(\xi_3), \qquad k = k(i, j)\,. \tag{17}$$

For $j = 1, 2$, $\varphi_j(\xi_3)$ are the regular linear shape functions. Given a particular order of approximation q in the "vertical" (ξ_3) direction, the functions $\varphi_j(\xi_3)$, $j = 1, \ldots, q-1$, coincide with the regular 1D Lagrange shape functions of order q, vanishing at the endpoints. Consequently, the mid-side and the middle node have two corresponding orders of approximation: a horizontal order p and a vertical order q. For the infinite element discretization, see [6]. Based on the convergence analysis for IFEM in [5], the IFEM approximation has been designed as an "overkill" in order to minimize the influence of the IFEM error on the FEM error in the coupled solution. We thus may assume that the errors measured in the annulus that is discretized by FEM are "pure" FEM errors. The error between the numerical and the exact solution is measured in the weighted H^1-norm in Ω^e, where

$$\|u - u_h\|^2_{1,\Omega^e} = \|u - u_h\|^2_{1,\Omega^e_s} + \|u - u_h\|^2_{1,\Omega_s}\,, \tag{18}$$

$$\|u - u_h\|^2_{1,\Omega^e_s} = \int_{\Omega^e_s} \frac{1}{r^2} |u - u_h|^2 \,\mathrm{d}\Omega^e_s + \int_{\Omega^e_s} \frac{1}{r^2} |\nabla(u - u_h)|^2 \,\mathrm{d}\Omega^e_s \tag{19}$$

and

$$\|u - u_h\|^2_{1,\Omega_s} = \int_{\Omega_s} |u - u_h|^2 \,\mathrm{d}\Omega_s + \int_{\Omega_s} |\nabla(u - u_h)|^2 \,\mathrm{d}\Omega_s\,. \tag{20}$$

The *best approximation error* in Ω_s is defined as

$$\inf_{u_h \in V_h(\Omega_s)} \|u - u_h\|_{H^1_w(\Omega_s)}\,, \tag{21}$$

where $V_h(\Omega_s) \subset H^1(\Omega_s)$ is the finite dimensional FE subspace of the Sobolev space $H^1(\Omega_s)$. The best approximation u_{ba} is defined uniquely and can be computed as the solution of

$$\begin{cases} \text{Find } u_{ba} \in V_h(\Omega_s) \quad \text{such that} \\ (u_{ba}, v_h)_{H^1(\Omega_s)} = (u, v_h)_{H^1(\Omega_s)} \qquad \forall\, v_h \in V_h(\Omega_s)\,, \end{cases} \tag{22}$$

where $(u, v)_{H^1(\Omega_s)}$ is the H^1-inner product

$$(u, v)_{H^1(\Omega_s)} = \int_{\Omega_s} \nabla u \cdot \nabla \overline{v} + u\overline{v} \,\mathrm{d}\Omega_s\,. \tag{23}$$

Computational results for this problem are shown in Table 1. We compute the relative FE and best approximation errors for the wavenumbers $k = 5$, 10, 20, 40. The mesh consists of $n = 1$, 2, 4 layers in radial direction with 24 prismatic elements in each layer. The polynomial degree in radial direction is $p = 2$, the degree in angular direction is $q = 4$. Convergence is explored by refinement in radial direction only; the angular discretization does not vary. The error curves are plotted in Fig. 9. Comparing to the one-dimensional results in Fig. 4, we see that the curves for lower k show a slight pollution effect but the FE-error is in the optimal range for $n = 4$, 8. On the other hand, the results for higher k show a significant pollution effect: on the maximal refinement possible (for this particular implementation), the FE error for $k = 40$ is still almost twice as large as the minimal error. Further refinement or p-enrichment would lead to asymptotic convergence as well. The results of additional computations will be published in [6].

Table 1. Best approximation error and Finite Element error in Ω_s in percent measured in the H^1-norm

l	k	$\frac{\|u-u_h^{ba}\|_{H^1_w(\Omega_s)}}{\|u\|_{H^1_w(\Omega_s)}}$	$\frac{\|u-u_h\|_{H^1_w(\Omega_s)}}{\|u\|_{H^1_w(\Omega_s)}}$
1	5	12.382	15.472
2		5.127	5.217
4		2.326	2.341
8		1.760	1.772
1	10	38.10	57.706
2		12.77	14.670
4		5.41	5.532
8		4.280	4.398
1	20	100.	100.
2		50.214	70.228
4		14.671	18.453
8		9.833	12.353
2	40	100.	100.
4		68.831	100.
8		20.943	39.4196

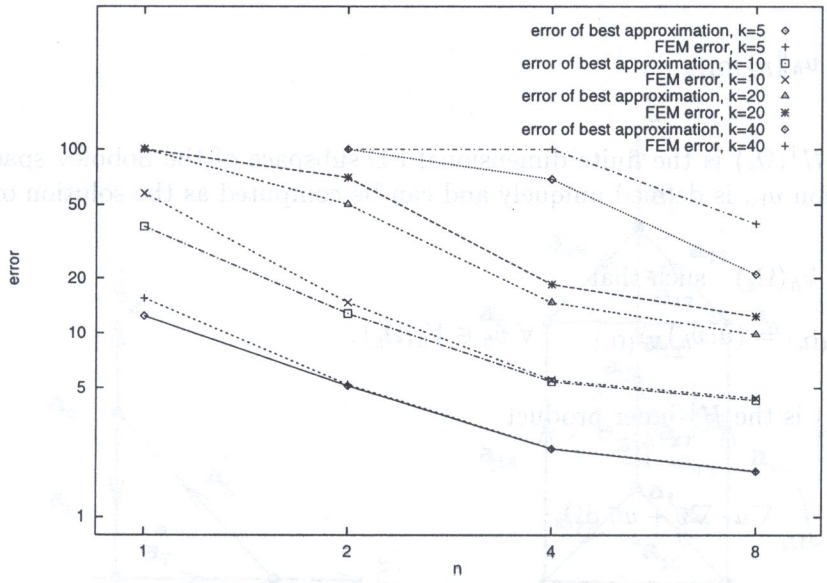

Fig. 9. Pollution effect in 3D-computations: Comparison of the optimal error and the finite element error for different k and radial refinement n

ACKNOWLEDGEMENTS

This paper is an expanded version of a talk that has been presented to the International conference "Ship Structure and Mechanics — Ultimate Capacity of Ship Structures" held at the Politechnika Szczecińska in memoriam of Prof. Dr. Marian Kmiecik on March 20-21, 1996. My teacher Professor Marian Kmiecik always urged me to maximally use the tools of mathematical and numerical analysis in the treatment of engineering problems. Years later, I found the ideal conditions for this

type of research in the laboratory of Prof. Ivo Babuška. My deepest gratitude goes to these persons as well as to Prof. Tinsley Oden for the invitation to the TICAM and Prof. Leszek Demkowicz for the introduction to his code and many fruitful discussions. The computational results shown in section 4 have been obtained jointly with Dr. Klaus Gerdes at TICAM. The local effectivity indices shown in section 3 have been computed by Mr. Srihari Gangaraj at Texas A&M University at College Station. The author is presently supported by the Grant Ih-23 of the Deutsche Forschungsgemeinschaft.

References

[1] I. Babuška, F. Ihlenburg, T. Strouboulis, S. Gangaraj. *A posteriori error estimation for FEM solution to Helmholtz's equation - part I: The quality of local indicators and estimators; part II: estimation of the pollution error.* TICAM Report, 96-32 and 96-33.

[2] I. Babuška, F. Ihlenburg, E. T. Paik, S. A. Sauter. A generalized finite element method for solving the Helmholtz equation in two dimensions with minimal pollution. *Comp. Methods Appl. Mech. Eng.*, **128**: 325–359, 1995.

[3] L. Demkowicz, W. Rachowicz, K. Banaś, J. Kucwaj. *2D hp adaptive package.* Technical report, Section of Applied Mathematics, Politechnika Krakowska, Cracow, 1992.

[4] L. Demkowicz, A. Bajer, K. Banaś. *Geometrical modeling package.* TICAM report 92–06, University of Texas at Austin, 1992.

[5] L. Demkowicz, K. Gerdes. *Convergence of the Infinite Element Methods for the Helmholtz Equation.* TICAM Report 95–07.

[6] K. Gerdes, F. Ihlenburg. *The pollution effect in FE solutions of the 3D Helmholtz equation with large wavenumber.* TICAM Report, 96-31.

[7] F. Ihlenburg, Error estimates for the Helmholtz equation, to appear in *ZAMM.*

[8] F. Ihlenburg, I. Babuška. Finite element solution to the Helmholtz equation with high wave number — part I: The *h*-version of the FEM. *Computers Math. Applic.*, **30**: 9–37, 1995.

[9] F. Ihlenburg, I. Babuška. Finite element solution to the Helmholtz equation with high wave number — part II: The *hp*-version of the FEM. Technical Note BN-1173, 1994, to appear in SIAM *J. Numer. Anal.*

[10] F. Ihlenburg, I. Babuška. Dispersion analysis and error estimation of Galerkin finite element methods for the Helmholtz equation. *Int. J. Num. Meth. Engng.*, **38**: 3745–3774, 1995.

[11] F. Ihlenburg, Ch. Makridakis. Error estimates of Galerkin FEM for a system of coupled Helmholtz equations in one dimension. In: W. Hackbusch, G. Wittum, eds., *Numerical treatment of coupled systems*, 96–105. Vieweg 1995.

[12] Ch. Makredakis, F. Ihlenburg, I. Babuška. Analysis and finite element methods for a fluid–solid interaction problem in one dimension. *Math. Methods and Models in Appl. Sciences*, to appear.

[13] L.L. Thompson, P.M. Pinsky. Complex wavenumber Fourier analysis of the *p*-version finite element method. *Computational Mechanics*, **13**: 255–275, 1994.

[14] O.C. Zienkiewicz, J.Z. Zhu. The superconvergent patch recovery and a posteriori error estimates. Part 1: The recovery technique. *Int. J. Num. Meth. Engng.*, **33**: 1331–1364, 1992.